Journal of Alloys and Compounds 501 (2010) 14–17

Contents lists available at ScienceDirect

Journal of Alloys and Compounds

journal homepage: www.elsevier.com/locate/jallcom

Synthesis and performance of high tap density $LiFePO_4$/C cathode materials doped with copper ions

Zhao-Rong Chang[a,*], Hao-Jie Lv[a], Hongwei Tang[a], Xiao-Zi Yuan[b], Haijiang Wang[b]

[a] *College of Chemistry and Environmental Science, Henan Normal University, Jianshe Road No. 46, Xinxiang, Henan 453007, PR China*
[b] *Institute for Fuel Cell Innovation, National Research Council of Canada, Vancouver, BC, Canada V6T 1W5*

ARTICLE INFO

Article history:
Received 19 February 2010
Received in revised form 24 March 2010
Accepted 15 April 2010
Available online 24 April 2010

Keywords:
Lithium ion battery
Cathode material
$LiFe_{1-x}Cu_xPO_4$
High tap density
Electrochemical performance

ABSTRACT

Stoichiometric Cu-doped lithium ion phosphate $LiFe_{1-x}Cu_xPO_4$/C ($x = 0$, 0.01, 0.015, 0.02, 0.025) cathode materials with a high tap density were synthesized by a solid state high temperature reaction in an inert atmosphere using $Cu(Ac)_2$ as a dopant and $FePO_4$ as a precursor. The synthesized $LiFe_{1-x}Cu_xPO_4$/C powders were characterized by X-ray diffraction (XRD), scanning electron microscopy (SEM) and electrochemical performance testing. The results indicate that the doped composite cathode materials are well crystallized with a typical homogeneous olivine-type structure. Materials with this olivine-type structure normally have a high crystallinity and high tap density. The tap density of $LiFe_{0.98}Cu_{0.02}PO_4$/C powders reached 1.98 g cm^{-3}. Charge–discharge test showed that the cathode materials possessed the excellent charge/discharge capacities, about 150 mAh g^{-1} and 297.0 mAh cm^{-3} at a rate of 0.1 C and more than 127.3 mAh g^{-1} and 252.1 mAh cm^{-3} at a rate of 2 C.

1. Introduction

In recent years, olivine-structured $LiFePO_4$ has attracted much attention as one of the most promising replacements of $LiCoO_2$ for lithium-ion batteries. Compared to commercial $LiCoO_2$, $LiNiO_2$, $LiMn_2O_4$, and their derivatives, $LiFePO_4$ cathode materials stand out due to several advantages, such as lower cost, excellent heat stability, lower toxicity, and fewer safety issues [1–3]. However, two main obstacles are preventing the commercialization of $LiFePO_4$. One is the poor electronic conductivity, which leads to an initial capacity loss and a poor rate capability of the material [4,5]. The other is the low tap density (1.0–1.3 g cm^{-3}), which results in a low volumetric specific capacity of the material [6].

Recently, a great deal of effort has been made to improve the electron conduction between particles of the material and the proton conduction of the internal crystal by doping carbon, metallic nano-particles and metallic ions [7–11]. Mi et al. [12] enhanced the discharge capacity of the material, $LiFePO_4$/(Ag + C), by adding Ag nano-particles while coating with carbon. Chiang et al. [13] obtained conductive materials of a p-type semiconductor by ion doping, and the conductivity reached 10^{-2} S cm^{-1}. Molenda et al. [14] reported that adding Mn in the synthesized $LiFePO_4$ material could greatly improve its conductivity. Wang et al. [15] used sucrose as a carbon source, and the product showed a capacity of 174 mAh g^{-1} at 0.1 C rate and around 117 mAh g^{-1} at 2 C rate with the capacity fading less than 10% after 50 cycles. Wu et al. [16] prepared and characterized Ti^{4+}-doped $LiFePO_4$ cathode materials, and found that $LiFe_{0.97}Ti_{0.03}PO_4$ manifested the most promising cycling performance when it was cycled with C/10, C/5, C/2, 1 C, 2 C, and 3 C rates. Furthermore, $LiFe_{0.97}Ti_{0.03}PO_4$ showed an initial discharge capacity of 135 mAh g^{-1}. These research results have demonstrated that a small amount of doping can, to some extent, improve the electrochemical performance of $LiFePO_4$. However despite the fact that tap density makes the most significant difference for increasing the specific energy density, an increase in the tap density of $LiFePO_4$ has rarely been reported. Based on our previous publications [17–19], $LiFe_{1-x}Cu_xPO_4$/C composite cathode material with a high tap density and conductivity for lithium-ion batteries was synthesized by using high tap density $FePO_4$ as a precursor, while adding $Cu(Ac)_2$ with different concentrations, and sintering under high temperature. The precursor was prepared by a ferric compound and glucose as a C source.

2. Experimental

2.1. Reagent and instrument

Reagents, such as H_3PO_4, $FeNO_3 \cdot 9H_2O$, Li_2CO_3, glucose and ammonia, used in this work are all of analytical grade. Other reagents include: polyvinylidene fluoride (PVDF, SCM Industrial Chemical Co., Ltd), n-methyl-2-pyrrolidone (NMP, Jing-Yu Fine Chemical Plant, Tianjin, China), and acetylene black (Jiachen Industrial Chemical, Shanghai, China).

Phase analysis and cell parameter determination of all samples were performed by X-ray diffraction (XRD) using a D8 X diffractometer (Germany, Bruker) with Cu

---

[*] Corresponding author. Tel.: +86 373 3326544; fax: +86 373 3326544.
E-mail address: czr_56@163.com (Z.-R. Chang).

0925-8388/$ – see front matter © 2010 Elsevier B.V. All rights reserved.
doi:10.1016/j.jallcom.2010.04.112

Kα radiation. The scan data were collected in the 2θ range of 10–80°. The step size was 0.026° with a counting time of 3 s. A scanning electron microscope (SEM) was used to examine the microstructures of the cathode material (SEM–XL30). The cells were tested on a Land CT2001A battery tester (Wuhan Jinnuo Electronics Co. Ltd., China) at 25 °C.

2.2. *Preparation of precursor $FePO_4$*

Stoichiometric amounts of H_3PO_4 and $FeNO_3 \cdot 9H_2O$ were dissolved in distilled water. To obtain the $FePO_4$ colloid, the dissolved aqueous solution was precipitated by adding an NH_3 solution of 5 mol dm^{-3}, under an argon atmosphere, with continuous stirring at 50 °C and a pH of 1.0–2.0. The co-precipitation mixture was then pressure-filtrated at 20 MPa, dried at 80 °C for 6 h, washed, dried again at 80 °C for 6 h, and ground, yielding the final precursor.

2.3. *Synthesis of cathode materials $LiFe_{1-x}Cu_xPO_4/C$*

The composite material $LiFe_{1-x}Cu_xPO_4/C$ was synthesized as follows. The obtained precursor powder $FePO_4$, Li_2CO_3, glucose and $Cu(Ac)_2$ with 1:0.5:0.1:0–0.025 molar ratio were mixed and ground. The mixture was initially heated under a 5% H_2–95% Ar_2 atmosphere, followed by sintering in a pipe furnace at 500 °C for 6 h, then at 750 °C for 18 h. After being heated, the products were cooled down to ambient temperature. Therefore then, the carbon coated and metallic ion doped final products, $LiFe_{1-x}Cu_xPO_4/C$ (x = 0, 0.01, 0.015, 0.02, 0.025), were obtained and marked as S1, S2, S3, S4, and S5.

The JZ-1 tap density tester (China) was used to determine the tap density of the sample. The procedure was as follows: (1) weighed the dried sample; (2) poured the weighed sample into the calibrated measuring cylinder; (3) installed the cylinder into the tester and operated it until the volume ceased to decrease; (4) read the volume. Then the tap density could be obtained.

2.4. *Electrochemical performance test*

Electrochemical characterization was performed on electrodes that were prepared as follows: a mixture of $LiFe_{1-x}Cu_xPO_4/C$, super P conductive carbon blacks, and a polyvinylidene fluoride (PVDF, Fluka), in a given ratio, was ground for 1 h in an agate mortar. Then *N*-methyl-2-pyrrolidone (NMP, Fluka) was added to the mixture by continuous grinding for another 1 h. The obtained slurry was spread on the aluminum current collector with a thickness of 12 μm, dried at 120 °C for 4 h under a vacuum (−0.1 MPa) atmosphere, and then pressed to form the cathode electrode. The electrode composition was 80 wt% $LiFe_{1-x}Cu_xPO_4/C$, 10 wt% acetylene black, and 10 wt% PVDF binder with an electrode area of 2.0 cm^2 and an active material loading of ca. 1–2 mg cm^{-2}. The coin cells (CR2016) were assembled with Li in excess as the counter electrode, Li as the reference electrode, and Celgard 2400 as the separator in an Ar-filled glove box. One mole per liter of $LiPF_6$ in ethylene carbonate (EC), diethyl carbonate (DEC), and dimethyl carbonate (DMC) (1:1:1, v/v) was used as the electrolyte solution. The cells were tested on a Land CT2001A battery tester (Wuhan Jinnuo Electronics Co. Ltd., China) at 25 °C. The charge–discharge experiment data were collected at current rates of 0.1–2 C (1 C is equivalent to 170 mAh g^{-1}) with a voltage range of 2.5–4.2 V versus Li/Li^+.

3. Results and discussion

3.1. *XRD analysis of the $FePO_4$ and $LiFe_{1-x}Cu_xPO_4/C$ powders*

Fig. 1 shows the XRD patterns of the synthesized $FePO_4$ powder with a high tap density of 1.56 g cm^{-3}. This figure reveals that the $FePO_4$ has the typical structure of a hexagonal α-$NaFeO_2$ type with a space group of $R\bar{3}m$. All the XRD peaks of the prepared precursor fit the standard $FePO_4$ spectrum (PDF#29-0715) well without impurities being detected. The lattice parameters are a = 0.5039 nm, b = 0.5039 nm, c = 1.1269 nm, and V = 0.2861 nm^3. This structure is conducive to the diffusion of lithium ions into the internal parts of the grains during the process of carbon thermo-reduction, forming an orthogonal olivine structure of $LiFePO_4$ with lithium ions along the c-axis in a straight line.

Fig. 2 shows the XRD patterns of the composite final product samples, and Table 1 shows their cell parameters. From Fig. 2 we can clearly see that no parasitic peaks are observable. All the diffraction peaks can be indexed from the orthorhombic structure with the space group of *Pnmb*, which is in agreement with a well-crystallized single phase $LiFePO_4$ according to PDF #40-1499. As can be seen in Table 1, cell parameters are close between doped and undoped samples. However, with increasing Cu content, a and c increase and b decreases. The ratio of the (1 1 1) peak and (3 1 1) peak (I_{111}/I_{311}) also rises as the doped Cu content increases. It reaches the maximum (0.9885), which is much higher than that of undoped $LiFePO_4/C$, when the doped Cu content is 2%. This is consistent with the results from the literature [20]. Table 1 also shows that tap density of samples increases with the value of I_{111}/I_{311}, which is obviously related to the high crystallinity of the material. As a result, the value of I_{111}/I_{311} is closely related to the electrochemical performance of Cu-doped $LiFePO_4$, and the higher the I_{111}/I_{311} value, the better the performance of the material. For Cu-doped $LiFePO_4$, Cu^{2+} ions might replace Li^+ ions in the 4a position of the octahedral $LiFePO_4$ crystal lattice. A slight change of cell parameters, which forms crystal defects, improves the electrical conductivity of the material due to the differences between the radius of Li^+ and Cu^{2+}.

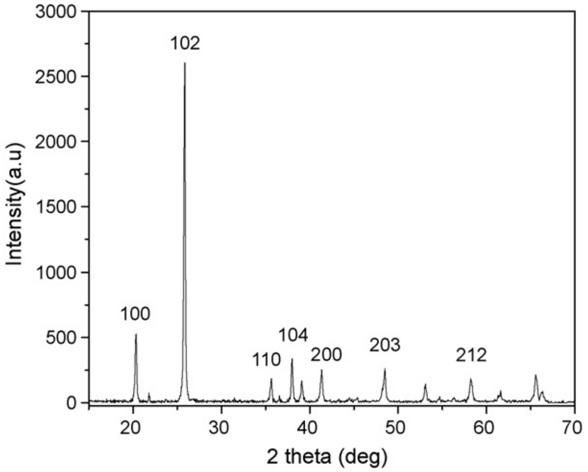

Fig. 1. XRD patterns of the precursor, $FePO_4$, synthesized by a two-step drying method.

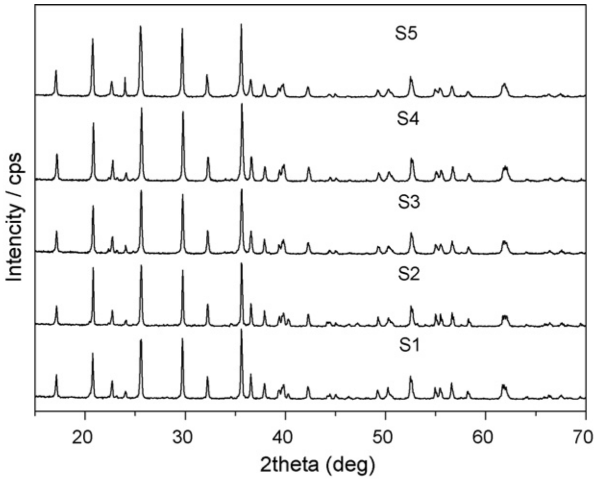

Fig. 2. XRD patterns of samples S1, S2, S3, S4, and S5.

Table 1
Lattice parameters and tap density for different Cu-doped $LiFePO_4$ samples.

Sample	a/nm	b/nm	c/nm	V/nm^3	I_{111}/I_{311}	Tap density/g cm^{-3}
S1	1.0336	0.6029	0.4702	0.2930	0.8531	1.94
S2	1.0320	0.6027	0.4672	0.2906	0.9639	1.95
S3	1.0332	0.6024	0.4692	0.2919	0.9884	1.98
S4	1.0333	0.6023	0.4692	0.2920	0.9885	1.98
S5	1.0333	0.6022	0.4694	0.2921	0.9873	1.97

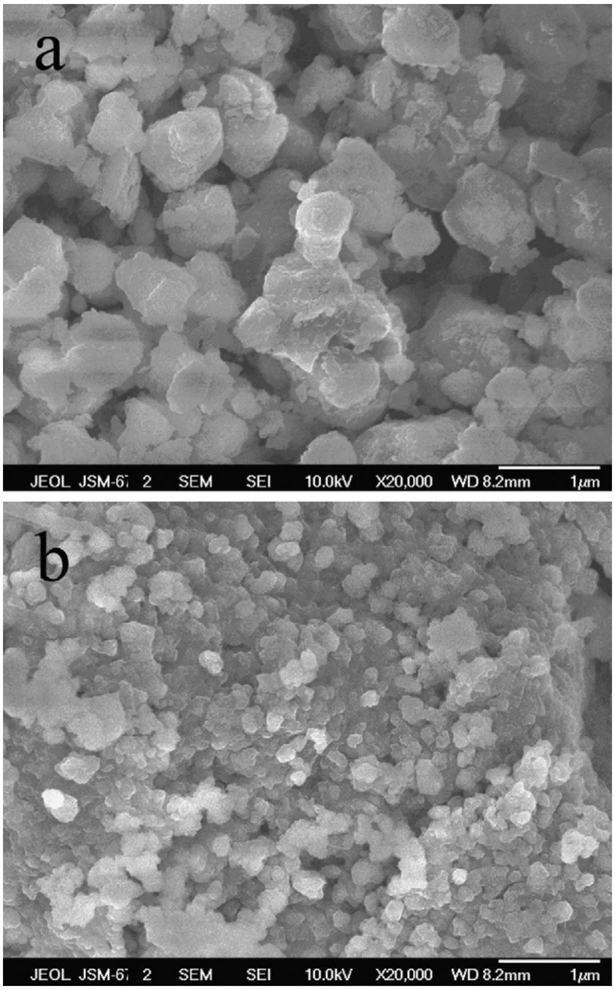

Fig. 3. SEM images of samples. (a)$LiFePO_4$/C; (b)$LiFe_{0.98}Cu_{0.02}PO_4$/C.

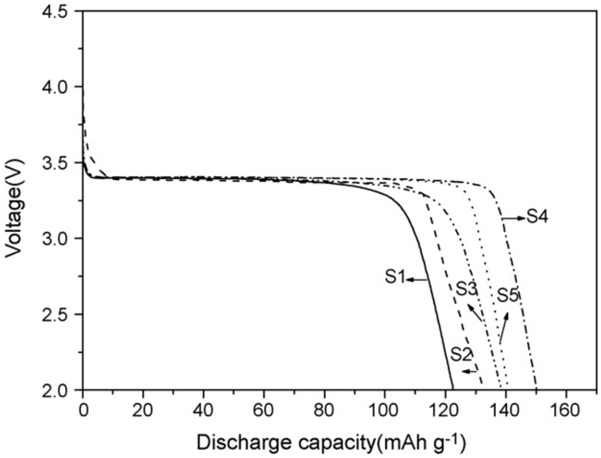

Fig. 4. Initial discharge curves for samples S1, S2, S3, S4, and S5 at 0.1 C.

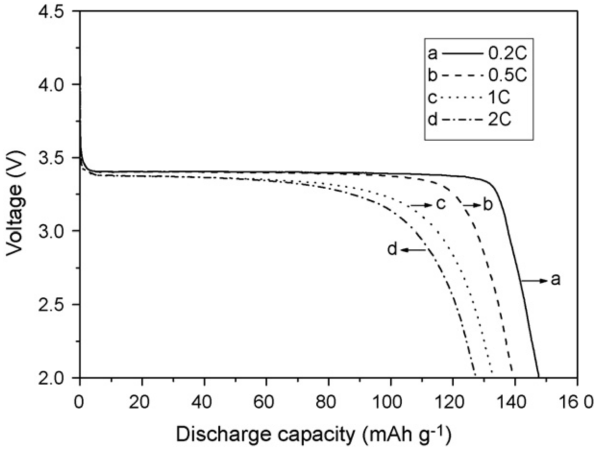

Fig. 5. Discharge curves of S4 at different rates.

3.2. *SEM analysis of $LiFePO_4$/C samples*

Fig. 3 shows the SEM images of the $LiFePO_4$/C sample, Fig. 3(a), and the $LiFe_{0.98}Cu_{0.02}PO_4$/C sample, Fig. 3(b). The particle size of Cu-doped $LiFePO_4$ is approximately ranging from 100 to 300 nm, which is smaller than that of Cu-undoped $LiFePO_4$ with the particle sizes ranging significantly, from 200 to 700 nm. This fact may indicate that Cu-doped $LiFePO_4$ plays an important role in the particle growth of $LiFePO_4$ particles during the synthesis process. The smaller size of the particle can expand contact between the electrolyte solution and sample surface, shortening the transmission channel in the solid-phase, and improving the insertion and extraction of Li-ions.

3.3. *Electrochemical characterization*

Fig. 4 shows the discharge capacity of each Cu-doped $LiFePO_4$/C sample at a rate of 0.1 C. Compared with undoped $LiFePO_4$/C material, the Cu-doped sample has a higher discharge capacity since the discharge capacity increases with increasing Cu^{2+} content. The initial discharge capacity of the undoped $LiFePO_4$/C sample is only 122.5 mAh g^{-1}, and the discharge voltage plateau is 3.4 V. When $x = 0.02$, the discharge capacity of sample S4 ($LiFe_{0.98}Cu_{0.02}PO_4$/C) reaches its maximum (150.0 mAh g^{-1}); when $x = 0.025$, it decreases to 138.3 mAh g^{-1}. This may be attributed to Cu^{2+} replacement of Li^+ in the 4a position of the octahedral $LiFePO_4$ crystal lattice. As a result, the slight change of cell parameters, which forms crystal defects, improves the electrical conductivity of the material due to the differences between the radii of Li^+ and Cu^{2+}. However, if the Cu content exceeds a certain level, the quantity of Li^+ will decrease in the process of charge and discharge, which lowers the electrochemical performance of the material.

To investigate the optimum working voltage and power output of the $LiFe_{0.98}Cu_{0.02}PO_4$/C composite powders, the lithium cells were discharged at different rates. Fig. 5 shows the discharge curves of the S4 sample ($LiFe_{0.98}Cu_{0.02}PO_4$/C) tested at different rates (0.2 C, 0.5 C, 1 C, 2 C). As can be seen, discharge plateau and discharge capacity decrease with increasing discharge rate. When the discharge rates increase from 0.2 and 0.5 C to 1 and 2 C, the discharge plateau decreases from 3.4 to 3.3 V as a result of the high discharge current density. At a discharge rate of 2 C, the discharge plateau reaches the minimum with a discharge capacity of 127.3 mAh g^{-1}. As the composite material possesses a high tap density (1.98 g cm^{-3}), a high volumetric capacity (252.1 mAh cm^{-3}) of the material is still achieved, which can greatly increase the energy density of batteries.

4. Conclusions

High tap density $LiFe_{1-x}Cu_xPO_4$/C powders were synthesized using $Cu(Ac)_2$ as a dopant and high tap density self-prepared $FePO_4$ as a precursor. The results indicate that Cu-doped $LiFePO_4$ particles can improve the discharge capacity and rate capability. At a discharge rate of 0.1 C, the initial discharge capacity of the high tap density $LiFe_{0.98}Cu_{0.02}PO_4/C$ is as high as 150.0 mAh g^{-1} and the specific volumetric capacity reaches 297.0 mAh cm^{-3}. At a discharge rate of 2 C, the initial discharge capacity is still over 127.3 mAh g^{-1} with a specific volumetric capacity of 252.1 mAh cm^{-3}. We conclude that Cu-doped $LiFePO_4$ with a Cu content of 0.02 is a promising cathode material for lithium ion batteries.

Acknowledgements

This work is financially supported by the Natural Science Foundation of China under approval No. 20671031, and by Henan Provincial Department of Science and Technology Key Research Project under approval No.080102270013.

References

[1] A.K. Padhi, K.S. Nanjundaswamy, J.B. Goodenough, J. Electrochem. Soc. 144 (1997) A1188–1194.
[2] A. Yamada, S.C. Chung, J. Electrochem. Soc. 148 (2001) A960–967.
[3] N. Terada, T. Yanagi, S. Arai, M. Yoshikawa, N. Nakajima, A. Yanai, N. Arai, J. Power Sources 100 (2001) 80–92.
[4] D. Morgan, A. Van der Ven, G. Ceder, Electrochem. Solid State Lett. 7 (2004) A30–32.
[5] M.S. Islam, D.J. Driscoll, C.A.J. Fisher, P.R. Slater, Chem. Mater. 17 (2005) 5085–5092.
[6] S.W. Oh, H.J. Bang, S.T. Myung, Y.C. Bae, S.M. Lee, Y.K. Sun, J. Electrochem. Soc. 155 (2008) A414–420.
[7] S. Franger, C. Benoit, C. Boarbon, F.L. Cars, J. Phys. Chem. Solids 67 (2006) 1338–1342.
[8] M.S. Song, Y.M. Kang, J.H. Kim, H.S. Kim, D.Y. Kim, H.S. Kwon, J.Y. Lee, J. Power Sources 166 (2007) 260–265.
[9] C.W. Kim, J.S. Park, K.S. Lee, J. Power Sources 163 (2006) 144–150.
[10] S.Y. Chung, J.T. Bloking, Y.M. Chiang, Nat. Mater. 1 (2002) 123–128.
[11] M. Rong, W.H. Ke, J. Electrochem. Soc. 155 (2008) A729–732.
[12] C.H. Mi, Y.X. Cao, X.G. Zhang, C.B. Zhao, H.L. Li, Powder Technol. 181 (2008) 301–306.
[13] W.G. Mcdonough, J.M. Antonucci, J.M. He, Y. Shimada, M.Y.M. Chiang, G.E. Schumacher, C.R. Schultheisz, Biomaterials 23 (2002) 3603–3608.
[14] J. Molenda, W. Ojczyk, J. Marzec, J. Power Sources 174 (2007) 689–694.
[15] K. Wang, R. Cai, T. Yuan, X. Yu, R. Ran, Z.P. Shao, Electrochim. Acta 54 (2009) 2861–2868.
[16] S.H. Wu, M.S. Chen, C.J. Chien, Y.P. Fu, J. Power Sources 189 (2009) 440–444.
[17] Z.R. Chang, H.J. Lv, H.W. Tang, H.J. Li, X.Z. Yuan, H.J. Wang, Electrochim. Acta 54 (2009) 4595–4599.
[18] Z.R. Chang, Z.J. Chen, F. Wu, H.W. Tang, Z.H. Zhu, X.Z. Yuan, H.J. Wang, Electrochim. Acta 53 (2008) 5927–5933.
[19] Z.R. Chang, Z.J. Chen, F. Wu, H.W. Tang, X.Z. Yuan, H.J. Wang, Electrochem. Solid State Lett. 11 (2008) A229–232.
[20] J.F. Ni, H.H. Zhou, J.T. Chen, J.Y. Su, Acta Phys.-Chim. Sin. 20 (2004) 582–586.